Inorganic Chemistry
Article

Inorg. Chem. **2009**, *48*, 5439–5448 **5439**
DOI: 10.1021/ic9004664

Stability and Reactivity of Grafted $Cr(CO)_3$ Species on MOF Linkers: A Computational Study

Jenny G. Vitillo,* Elena Groppo, Silvia Bordiga, Sachin Chavan, Gabriele Ricchiardi, and Adriano Zecchina

Dipartimento di Chimica IFM and NIS Centre of Excellence, Università di Torino, INSTM UdR Università, Via Pietro Giuria 7, 10125 Torino, Italia

Received March 9, 2009

The possibility to modulate $Cr(CO)_3$ properties by grafting it onto metal-organic framework (MOF) linkers of different natures has been investigated using density functional methods. MOF linkers were modeled using clusters constituted by benzene rings doubly substituted in the para position. The effect of the electron-donor or electron-acceptor nature of benzene substituents on the stability of the (η^6-arene)$Cr(CO)_3$ adduct and on the shift of the CO bands has been considered. Different electron-donor ($-NH_2$, $-CH_3$, $-OH$, $-COONa$) and electron-acceptor ($-F$, $-COOH$, $-CN$, $-CF_3$) substituents have been used and the results compared with the bare benzene. $C_6H_4(COOZnOH)_2$ and $C_6H_4(Zn_4O_{13}C_6H_5)_2$ clusters have also been adopted as models of the MOF-5 benzene rings. The possibility of modulating the stability and the reactivity of $Cr(CO)_3$ species by grafting them to MOFs with different organic linkers was verified. In particular, this study indicates that electron-acceptor (e.g., $C_6H_4(COOH)_2$) substituted MOF linkers facilitate the substitution of CO by incoming molecules, whereas the use of electron-donor ones (e.g., $C_6H_4(OH)_2$) would improve the stability of the $Cr(CO)_3$ adduct and the ring acidity. Furthermore, an almost linear dependence of the $Cr(CO)_3$ binding energies on the calculated structural and vibrational features of the tricarbonyl was found, suggesting that the stability of the $Cr(CO)_3$ adduct can be inferred experimentally from vibrational and diffraction data. In the end, on the basis of the results obtained, it was possible to successfully explain the experimental shift of the CO IR stretching features of grafted $Cr(CO)_3$ on the UiO-66, CPO-27-Ni, and MOF-5 aromatic linkers and on the benzene rings of poly(ethylstyrene-*co*-divinylbenzene). The sign of the $\Delta\tilde{\nu}_{CO}$ shift with respect to $C_6H_6Cr(CO)_3$ has been found to be strongly dependent on higher/lower electron density on the ring.

I. Introduction

The conceptual easiness of metal-organic framework (MOF) materials design represents one of their attractive features for what concerns their potential applications in the gas storage[1,2] and catalysis fields.[3] Unfortunately, the introduction of open metal sites in the structure during synthesis, when possible, has some drawbacks: first of all, none of the MOFs having a metal site in their structure presents, to our knowledge, more than one coordination vacancy per site. Moreover, being synthesized in solution, the open metal sites after the synthesis are not actually free but they do not present a coordination vacancy but coordinate a solvent molecule:[4,5] in this case, the temperature of the solvent desorption has to be lower than the onset temperature of the MOF decomposition. The possibility of creating open metal sites or catalytically active species in MOF materials in postsynthesis processes represents a valuable alternative. Recently, Kaye and Long have succeeded in grafting $Cr(CO)_3$ species on benzene rings of MOF-5.[6] The (η^6-arene)$Cr(CO)_3$'s are interesting compounds for essentially two reasons: first, they serve as building blocks in organometallic chemistry and play important roles in heterogeneous catalysis.[7−11] Moreover, $M(CO)_n$ coordination entities (M = Cr, Mo and W, $n \leq 6$) undergo UV light-activated substitution of a CO ligand by N_2 or H_2, as demonstrated in solution studies,[12] matrix

*To whom correspondence should be addressed. E-mail: jenny.vitillo@unito.it.

(1) Ma, S. Q.; Sun, D. F.; Simmons, J. M.; Collier, C. D.; Yuan, D. Q.; Zhou, H. C. *J. Am. Chem. Soc.* **2008**, *130*, 1012–1016.
(2) Han, S. S.; Furukawa, H.; Yaghi, O. M.; Goddard, W. A. *J. Am. Chem. Soc.* **2008**, *130*, 11580–11581.
(3) Horcajada, P.; Surble, S.; Serre, C.; Hong, D. Y.; Seo, Y. K.; Chang, J. S.; Greneche, J. M.; Margiolaki, I.; Ferey, G. *Chem. Commun.* **2007**, 2820–2822.
(4) Prestipino, C.; Regli, L.; Vitillo, J. G.; Bonino, F.; Damin, A.; Lamberti, C.; Zecchina, A.; Solari, P. L.; Kongshaug, K. O.; Bordiga, S. *Chem. Mater.* **2006**, *18*, 1337–1346.
(5) Vitillo, J. G.; Regli, L.; Chavan, S.; Ricchiardi, G.; Spoto, G.; Dietzel, P. D. C.; Bordiga, S.; Zecchina, A. *J. Am. Chem. Soc.* **2008**, *130*, 8386–8396.
(6) Kaye, S. S.; Long, J. R. *J. Am. Chem. Soc.* **2008**, *130*, 806–807.
(7) Roald, H. *Angew. Chem., Int. Ed.* **1982**, *21*, 711–724.
(8) Soderberg, B. C. G. *Coord. Chem. Rev.* **2008**, *252*, 57–133.
(9) Rosillo, M.; Dominguez, G.; Casarrubios, L.; Perez-Castells, J. *J. Org. Chem.* **2005**, *70*, 10611–10614.
(10) Schellhaas, K.; Schmalz, H. G.; Bats, J. W. *Chem. Eur. J.* **1998**, *4*, 57–66.
(11) Kim, J.; Kim, T. K.; Kim, J.; Lee, Y. S.; Ihee, H. *J. Phys. Chem. A* **2007**, *111*, 4697–4710 and refs therein.
(12) Upmacis, R. K.; Poliakoff, M.; Turner, J. J. *J. Am. Chem. Soc.* **1986**, *108*, 3645–3651.

© 2009 American Chemical Society
Published on Web 05/12/2009

isolation experiments,[13] and supercritical fluids.[14] This ability is maintained if the (η^6-arene)$Cr(CO)_3$ is isolated in a polyethylene matrix[15] or the $Cr(CO)_3$ species are grafted on the structural MOFs' benzene rings,[6] with potential applications in the hydrogen storage field. Zheng et al.[16] succeeded in decomposing the (η^6-C_6H_6)$Cr(CO)_3$ complex in (η^6-C_6H_6)-Cr(CO) by performing 266 nm UV irradiation. (η^6-C_6H_6)-Cr(CO) is very interesting because the Cr atom possesses two coordination vacancies. If the same decomposition reaction would be achieved in MOFs, this could allow the creation of metal sites having two coordination vacancies, with important implications, in particular, in the gas storage and catalysis fields.

The properties and stability of the $Cr(CO)_3$ moiety are strongly influenced by the π-properties of the arene linker: a change in some of the arene substituents affects the overall (arene)$Cr(CO)_3$ system. The effect of electron-donating and electron-accepting arene substituents in (η^6-arene)$Cr(CO)_n$ (n = 1−3) on the chemical shifts[17] and geometrical[18,19] and vibrational[14,17,19] properties of the $Cr(CO)_3$ tripod have been previously studied both experimentally[14,17,18] and computationally.[19] Moreover, very recently, Head-Gordon and coworkers[20] have explored by computational techniques the effect of π-donating and π-accepting arene substituents in (η^6-arene)$Cr(CO)_{3-n}(H_2)_n$ (n = 1−3) on the M−H_2 binding interaction. However, to our knowledge, a systematic study aimed at underlining the effect of the benzene substituents' nature on the C−O vibrational properties and identifying the correlations existing between the structural and vibrational properties of the (η^6-arene)$Cr(CO)_3$ adducts with the energetic of the Cr−CO and Cr−arene bonds is still lacking. The reliability of atomistic modeling of MOFs and their importance in addressing the experiments have been the topic of a recent review.[21]

In this study, quantum mechanical methods have been used to characterize the effect of electron-donating and electron-accepting arene substituents on the stability and vibrational properties of the (η^6-arene)$Cr(CO)_3$ adducts. Different p-$C_6H_4X_2$ arene species have been considered (see Scheme 1a), where X = −H for benzene; $-CH_3$, −OH, and $-NH_2$ as electron-donor substituents; or −F, −CN, and $-CF_3$ as electron-acceptor substituents. These functional

Scheme 1

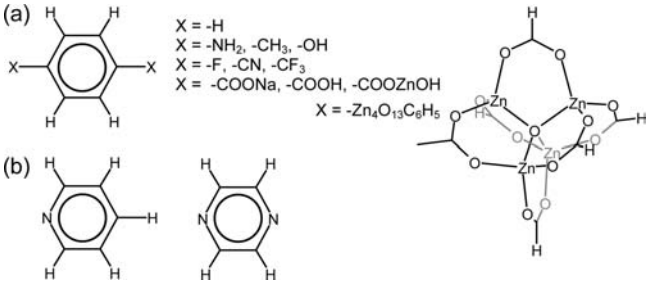

groups are often present in MOFs' linkers.[22−28] C_5H_5N and $C_4H_4N_2$ have been also considered (see Scheme 1b) in order to verify the effect of the presence of the N heteroatom in the ring. This has been done not only because C_5H_5N and $C_4H_4N_2$ are common organic linkers in MOFs[22,27,29−32] but also because the $Cr(CO)_3$ complex on pyridine is the only case, to our knowledge, where the complete replacement of the three CO ligands by N_2 molecules was observed.[15] Finally, the p-$C_6H_4(COOH)_2$, p-$C_6H_4(COONa)_2$, p-C_6H_4-$(COOZnOH)_2$, and p-$C_6H_4(Zn_4O_{13}C_6H_5)_2$ molecules have been taken into account as models of the MOF-5 benzene rings with increasing degrees of complexity.

All of the complexes have been studied with three density functional methods having the same correlation functional but different exchange functionals characterized by a different proportion of Hartree−Fock (HF) exchange (BLYP, B3LYP, and BHandHLYP), with the aim of verifying the effect of the HF exchange proportion on the computed quantities. Moreover, the use of functionals with different proportions of HF exchange is suggested in order to avoid bias of the method when different spin-state energy surfaces are compared, a comparison that cannot be avoided in decomposition studies of the (η^6-arene)$Cr(CO)_3$ complexes.[33−37] Finally, the BP86 method has been also used, because it is a widely used density functional with a good performance-to-cost ratio, and is known for its consistent and reliable prediction of geometry, vibrational frequencies, and bond energies of transition metal complexes.[20,38]

The formation enthalpy of all of the adducts has been analyzed as a function of the Cr−arene and Cr−CO distances

(13) Sweany, R. L. *J. Am. Chem. Soc.* **1985**, *107*, 2374.
(14) Howdle, S. M.; Healy, M. A.; Poliakoff, M. *J. Am. Chem. Soc.* **1990**, *112*, 4804–4813.
(15) Goff, S. E. J.; Nolan, T. F.; George, M. W.; Poliakoff, M. *Organometallics* **1998**, *17*, 2730–2737.
(16) Zheng, Y. F.; Wang, W. H.; Lin, J. G.; She, Y. B.; Fu, K. J. *J. Phys. Chem.* **1992**, *96*, 9821–9827.
(17) Hunter, A. D.; Mozol, V.; Tsai, S. D. *Organometallics* **1992**, *11*, 2251–2262.
(18) Hunter, A. D.; Shilliday, L.; Furey, W. S.; Zaworotko, M. J. *Organometallics* **1992**, *11*, 1550–1560.
(19) Suresh, C. H.; Koga, N.; Gadre, S. R. *Organometallics* **2000**, *19*, 3008–3015.
(20) Lochan, R. C.; Khaliullin, R. Z.; Head-Gordon, M. *Inorg. Chem.* **2008**, *47*, 4032–4044.
(21) Keskin, S.; Liu, J.; Rankin, R. B.; Johnson, J. K.; Sholl, D. S. *Ind. Eng. Chem. Res.* **2009**, *48*, 2355–2371.
(22) Chun, H.; Dybtsev, D. N.; Kim, H.; Kim, K. *Chem. Eur. J.* **2005**, *11*, 3521–3529.
(23) Rowsell, J. L. C.; Yaghi, O. M. *J. Am. Chem. Soc.* **2006**, *128*, 1304–1315.
(24) Rowsell, J. L. C.; Millward, A. R.; Park, K. S.; Yaghi, O. M. *J. Am. Chem. Soc.* **2004**, *126*, 5666–5667.
(25) Munakata, M.; Ning, G. L.; Kuroda-Sowa, T.; Maekawa, M.; Suenaga, Y.; Horino, T. *Inorg. Chem.* **1998**, *37*, 5651–5656.
(26) Eddaoudi, M.; Kim, J.; Rosi, N.; Vodak, D.; Wachter, J.; O'Keeffe, M.; Yaghi, O. M. *Science* **2002**, *295*, 469–472.
(27) Dybtsev, D. N.; Chun, H.; Kim, K. *Angew. Chem., Int. Ed.* **2004**, *43*, 5033–5036.
(28) Furukawa, H.; Kim, J.; Ockwig, N. W.; Keeffe, M.; Yaghi, O. M. *J. Am. Chem. Soc.* **2008**, *130*, 11650–11661.
(29) Szeto, K. C.; Kongshaug, K. O.; Jakobsen, S.; Tilset, M.; Lillerud, K. P. *Dalton Trans.* **2008**, 2054–2060.
(30) Lee, E. Y.; Suh, M. P. *Angew. Chem., Int. Ed.* **2004**, *43*, 2798–2801.
(31) Kitaura, R.; Kitagawa, S.; Kubota, Y.; Kobayashi, T. C.; Kindo, K.; Mita, Y.; Matsuo, A.; Kobayashi, M.; Chang, H. C.; Ozawa, T. C.; Suzuki, M.; Sakata, M.; Takata, M. *Science* **2002**, *298*, 2358–2361.
(32) Noro, S.; Kitagawa, S.; Nakamura, T.; Wada, T. *Inorg. Chem.* **2005**, *44*, 3960–3971.
(33) Cohen, R.; Weitz, E.; Martin, J. M. L.; Ratner, M. A. *Organometallics* **2004**, *23*, 2315–2325.
(34) McGrady, J. E.; Dyson, P. J. *J. Organomet. Chem.* **2000**, *607*, 203–207.
(35) Li, Y.; McGrady, J. E.; Baer, T. *J. Am. Chem. Soc.* **2002**, *124*, 4487–4494.
(36) Poater, J.; Sola, M.; Rimola, A.; Rodriguez-Santiago, L.; Sodupe, M. *J. Phys. Chem. A* **2004**, *108*, 6072–6078.
(37) Estephane, J.; Groppo, E.; Vitillo, J. G.; Damin, A.; Lamberti, C.; Bordiga, S.; Zecchina, A. *Phys. Chem. Chem. Phys.* **2009**, *11*, 2218–2227.
(38) Ahlrichs, R.; Furche, F.; Grimme, S. *Chem. Phys. Lett.* **2000**, *325*, 317–321.

and of the CO stretching frequencies. The final goal was to establish a relation between the stability of the (η^6-arene)-$Cr(CO)_3$ adducts and experimentally valuable quantities, as obtained by X-ray diffraction (XRD), X-ray absorption spectroscopies, or Fourier-transformed infrared (FTIR) spectroscopy. In particular, the calculated vibrational properties were compared directly with a set of new experimental data obtained upon the formation of grafted $Cr(CO)_3$ units on arene rings present as structural elements in highly porous materials. The aim is to ascertain whether the computational methods can help in the design of the MOFs' organic linkers to facilitate the adsorption of the $Cr(CO)_3$ species or to increase or decrease the stability of the grafted chromium tricarbonyl exploiting the flexibility of the MOF synthesis. Indications about what linker could facilitate the CO substitution by incoming molecules could also be obtained.[20] Finally, the electrostatic potential (ESP) of the rings has also been evaluated in order to help in the understanding of the diverse trends obtained for the different arene families. In particular, the ESP maps were helpful in the understanding and prediction of the (η^6-arene)$Cr(CO)_3$ complexes' stability and of the activation of the Cr−CO bond.[19]

II. Methods

II.A. Theoretical Calculations. The calculations have been performed with the *Gaussian 03* software package.[39] All of the systems under study have been optimized by the BP86, BLYP, B3LYP, and BHandHLYP methods. BP86 is a pure-DFT method, combining Becke's 1988 exchange functional,[40] which includes the Slater exchange along with corrections involving the gradient of the density and the gradient corrections of Perdew, along with his 1981 local correlation functional.[41] Three Hamiltonians having the same correlation functional (Lee, Yang, and Parr's gradient-corrected correlation functional, LYP)[42] but different exchange functionals have been used in order to evaluate the effect of the exchange part and, in particular, of the different proportions of HF exchange (X_{HF}) on the computed quantities: BLYP (with Becke's 1988 exchange functional, $X_{HF} = 0$),[40] B3LYP (with Becke's three-parameter hybrid exchange functional, $X_{HF} = 0.2$),[43] and BHandHLYP (half-and-half functionals as implemented in *Gaussian 03*,[36,39] $X_{HF} = 0.5$). BP86 has $X_{HF} = 0$. Unrestricted formalisms have been used in all cases, except for the singlet state. The restricted formalism has been preferred for the singlet state in order to avoid artifacts due to spin contamination.[11]

For the hydrogen atoms, the standard Pople basis set supplemented by diffuse and polarizability functions 6-311++G(2d,2p) has been adopted.[44,45] The Na and Zn elements have been modeled by means of the fully optimized triple-ζ valence basis sets proposed by Ahlrichs et al.[46] supplemented by polarization (TZVp). For all of the other elements, the TZV basis set has been augmented by two sets of polarization functions derived from the original ones following an even-tempered recipe that substitutes the polarization orbital in the basis set with two orbitals, having respectively the coefficient doubled and halved with respect to the parent orbital. The so-obtained basis sets will be indicated as TZV2p.

Geometry optimization has been carried out by means of the Berny optimization algorithm with an analytical gradient. The thresholds were set to 0.000450 and 0.000300 au for the maximum and the rms forces, respectively, and to 0.001800 and 0.001200 au for the maximum and rms atomic displacements, respectively. A (99, 590) pruned grid was used (i.e., 99 radial points and 590 angular points per radial point). No geometrical constraints have been imposed. No symmetry constraints have been imposed for clusters having a spin multiplicity higher than one.

Harmonic frequencies have been obtained by analytically determining the second derivatives of the energy with respect to the Cartesian nuclear coordinates and then transforming to mass-weighted coordinates. No scaling factor has been adopted. The dissociation energy from the ground state (D_0) of the adducts was calculated from the corresponding dissociation energy from the potential energy minimum D_e for the reaction

$$(\eta^6\text{−arene})Cr(CO)_3 \rightleftharpoons \text{arene} + Cr(CO)_3 \qquad (1)$$

by including the zero-point energies (ZPE) of reactants and products. The ZPE was calculated in the harmonic approximation. The enthalpy variations ($\Delta H_{Cr(CO)_3}$) under standard conditions (298.15 K and 1 atm) were derived from the reaction energies including the ZPE and temperature corrections. The temperature corrections were computed using the standard expressions for an ideal gas in the canonical ensemble. No scaling factors were adopted.

The determination of the spin state of the bare $Cr(CO)_3$ tripod in its ground state is still an unresolved computational task, not only for the DFT functionals but also for the CC methods.[11] This is due to the well-known problem of modeling of transition metals[11,33,36] and, more specifically, to the high-spin contamination obtained when open-shell configurations of $Cr(CO)_3$ are considered (that is, for $2S + 1 > 1$).[33] However, on the experimental side, evidence of the singlet state and C_{3v} symmetry of such a tripod has been obtained.[11] In the present work, all of the methods but BHandHLYP agree with the experimental indications and previous calculations.[11] BHandHLYP, on the contrary, suggested the tripod to be in the triplet state (more stable than the singlet state by 61 kJ/mol). However, this calculation was characterized by a strong spin contamination in the triplet state ($S^2 = 2.77$ after annihilation versus a theoretical value of 2).[11] For that reason, the BHandHLYP results for $Cr(CO)_3$ in the triplet state were disregarded. In order to have an estimation of the bond strength between the arenes and the tripod and the stability of such complexes, the reference state of the $Cr(CO)_3$ unit has been considered the singlet state.

The enthalpy variation ($\Delta H_{Cr(CO)_6}$) of the grafting reaction,

$$\text{arene} + Cr(CO)_6 \rightleftharpoons (\eta^6\text{−arene})Cr(CO)_3 + 3CO \qquad (2)$$

was also evaluated under standard conditions.

(39) Frisch, M. J.; Trucks, G. W.; Schlegel, H. B.; Scuseria, G. E.; Robb, M. A.; Cheeseman, J. R.; Montgomery, J., J. A.; Vreven, T.; Kudin, K. N.; Burant, J. C.; Millam, J. M.; Iyengar, S. S.; Tomasi, J.; Barone, V.; Mennucci, B.; Cossi, M.; Scalmani, G.; Rega, N.; Petersson, G. A.; Nakatsuji, H.; Hada, M.; Ehara, M.; Toyota, K.; Fukuda, R.; Hasegawa, J.; Ishida, M.; Nakajima, T.; Honda, Y.; Kitao, O.; Nakai, H.; Klene, M.; Li, X.; Knox, J. E.; Hratchian, H. P.; Cross, J. B.; Bakken, V.; Adamo, C.; Jaramillo, J.; Gomperts, R.; Stratmann, R. E.; Yazyev, O.; Austin, A. J.; Cammi, R.; Pomelli, C.; Ochterski, J. W.; Ayala, P. Y.; Morokuma, K.; Voth, G. A.; Salvador, P.; Dannenberg, J. J.; Zakrzewski, V. G.; Dapprich, S.; Daniels, A. D.; Strain, M. C.; Farkas, O.; Malick, D. K.; Rabuck, A. D.; Raghavachari, K.; Foresman, J. B.; Ortiz, J. V.; Cui, Q.; Baboul, A. G.; Clifford, S.; Cioslowski, J.; Stefanov, B. B.; Liu, G.; Liashenko, A.; Piskorz, P.; Komaromi, I.; Martin, R. L.; Fox, D. J.; Keith, T.; Al-Laham, M. A.; Peng, C. Y.; Nanayakkara, A.; Challacombe, M.; Gill, P. M. W.; Johnson, B.; Chen, W.; Wong, M. W.; Gonzalez, C.; Pople, J. A. *Gaussian 03*, revision B.05; Gaussian, Inc.: Wallingford, CT, **2004**.
(40) Becke, A. D. *Phys. Rev. A* **1988**, *38*, 3098–3100.
(41) Perdew, J. P. *Phys. Rev. B* **1986**, *33*, 8822–8824.
(42) Lee, C.; Yang, W.; Parr, R. G. *Phys. Rev. B* **1988**, *37*, 785–789.
(43) Becke, A. D. *J. Chem. Phys.* **1993**, *98*, 5648–5652.
(44) Clark, T.; Chandrasekhar, J.; Spitznagel, G. W.; Schleyer, P. v. R. *J. Comput. Chem.* **1983**, *4*, 294.
(45) Frisch, M. J.; Pople, J. A.; Binkley, J. S. *J. Chem. Phys.* **1984**, *80*, 3265–3269.
(46) Schafer, A.; Huber, C.; Ahlrichs, R. *J. Chem. Phys.* **1994**, *100*, 5829–5835.

All of the energetic data have been corrected for the basis set superposition error (BSSE) affecting the (η^6-arene)$Cr(CO)_3$ energy following the a posteriori method proposed by Boys and Bernardi[47] as implemented in *Gaussian 03*. The BSSE-corrected energetic values are signaled by a "c" superscript and were obtained from the computed Y values as $Y^c = Y - BSSE$. In all cases, the BSSE correction to the energy was found to be less than the 5% of the adduct binding energy.

Charge transfer from the arenes to the $Cr(CO)_3$ tripod has been estimated using the Mulliken population analysis.[48]

II.B. Experimental Details. IR spectra have been obtained in transmission mode on a Bruker IFS66 instrument, equipped with an MCT detector, at a resolution of 2 cm^{-1}. Self-supported pellets of three different materials have been investigated: a microporous poly(ethylstyrene-*co*-divinylbenzene)[49] polymer (indicated as PS in the following); UiO-66,[50] a MOF with no exposed metal sites; and CPO-27-Ni,[5] a MOF material with exposed Ni^{2+} sites. The samples were activated in vacuum in order to remove all of the adsorbates (solvents and water). Details on the materials' structure and on the activation conditions can be found in refs 51 and 50 and 5, respectively. $Cr(CO)_6$ has been dosed from the gas phase by sublimation of the solid and the samples treated in a controlled atmosphere at temperatures below 150 °C (temperature where the decomposition of the $Cr(CO)_6$ starts) in order to optimize the formation of the (η^6-arene)$Cr(CO)_3$ species. In particular, grafted $Cr(CO)_3$ species inside PS were formed upon heating $Cr(CO)_6$/PS in a closed reactor at 150 °C for 14 h, followed by the removal of the gas phase. The formation of grafted $Cr(CO)_3$ species inside UiO-66 has been obtained upon heating $Cr(CO)_6$/UiO-66 at 150 °C for 14 h in a reactor under pumping. In the case of the $Cr(CO)_6$/CPO-27-Ni system, the completion of the grafting reaction has been achieved after heating and outgassing $Cr(CO)_6$/CPO-27-Ni at 120 °C for only 30 min. For comparison, the IR spectrum of the (η^6-C_6H_6)$Cr(CO)_3$ compound (Sigma Aldrich) dispersed in nujol has been also obtained. For further details, please refer to ref 49.

III. Results and Discussion

The coordinates of all of the systems considered in this paper and obtained at the B3LYP level have been reported in the Supporting Information. All of the systems have been verified to be minima of the potential energy surface, except when otherwise specified. For the $-CH_3$ (and the $-CF_3$) system, the reference bare arene has been chosen to be that with the $-CH_3$ (and $-CF_3$) units in the eclipsed conformation (although slightly higher in energy with respect to the corresponding staggered conformation and characterized in the $-CH_3$ case by an imaginary mode at about 15i cm^{-1}), and the $Cr(CO)_3$ has been placed on the side with two H's (or F's) of the $-CH_3$ groups. As for the $Cr(CO)_3$ complex, the trans conformer of *p*-$C_6H_4(OH)_2$ was the more stable by 0.2 kJ/mol (according to B3LYP) than the corresponding cis conformer; for this reason, the considered reference arene was the trans *p*-$C_6H_4(OH)_2$.

In the following, only the results obtained at the B3LYP and BP86 levels are reported. The corresponding tables and plots for the BLYP and BHandHLYP methods are contained in the Supporting Information.

III.A. Isolated Arenes. The ESP maps on the optimized structure of the arenes have been evaluated, at all levels of calculation, giving indistinguishable results. The maps obtained at the B3LYP level are reported in Figure 1, while the structures are shown in Figure S1 (Supporting Information). The electrostatic potential on the ring was quite influenced by the presence of substituents or heteroatoms. In particular, for electron-acceptor substituted benzene, the rings were characterized by positive values of the ESP. An increase in the positive character of the ESP on the ring has also been observed for C_5H_5N and $C_4H_4N_2$ and correlated with the higher electronegativity of nitrogen with respect to carbon atoms. On the contrary, for benzene, the ESP assumes negative values on the ring, while more negative values are observed for π-donor substituted benzenes.[52] This agrees with what was expected on the basis of qualitative considerations. The only exception was *p*-$C_6H_4(OH)_2$, where the ESP assumed less negative values on the ring with respect to benzene. Finally, the effect on ESP was additive with respect to the number of heteroatoms (see Figure 1) and substituents on the ring, in agreement with previous findings.[17]

Coming to the four cluster models utilized for the modeling of the MOF-5 benzene rings, *p*-$C_6H_4(COOH)_2$, *p*-$C_6H_4(COOZnOH)_2$, and $C_6H_4(Zn_4O_{13}C_6H_5)_2$ showed a positive potential on the ring, in agreement with previous calculations on a periodic MOF-5 model.[5] On the contrary, *p*-$C_6H_4(COONa)_2$ resulted to be the arene characterized by the most negative values of ESP on the ring, likely due to the presence of the Na^+ cations, which causes the presence of a small negative charge on the ring ($q_{Mulliken} = -0.19e$). As a consequence, the *p*-$C_6H_4(COONa)_2$ model is not able to correctly reproduce the electrostatic properties of benzene rings of MOF-5.

III.B. (η^6-Arene)$Cr(CO)_3$. The main geometrical, vibrational, and energetic features of the $Cr(CO)_3$ and $Cr(CO)_6$ molecules are contained in the Supporting Information, while those of the (η^6-arene)$Cr(CO)_3$ complexes are reported in Tables 1 and 2 (the data obtained at the BLYP and BHandHLYP levels are reported in Tables S5 and S7, Supporting Information). At all levels, the ground state was confirmed to be the singlet state, in agreement with previous calculations.[33]

In order to simplify the discussion in the following, all of the (η^6-arene)$Cr(CO)_3$ complexes under study have been divided into two groups (excluding benzene), according to the ESP potential values on the ring: the PA set if positive and the NA set if negative.

III.B.1. Geometrical Properties. Possible conformations of the $Cr(CO)_3$ tripod relative to the ring carbon atoms and substituents (or heteroatoms) are depicted in Scheme 2.

Staggered (a) and eclipsed (b) conformations can be identified in all cases, while for monosubstitued benzene

(47) Boys, S. F.; Bernardi, F. *Mol. Phys.* **1970**, *19*, 553–566.
(48) Mulliken, R. S. *J. Chem. Phys.* **1955**, *23*, 1833–1840.
(49) Chavan, S. Manuscript in preparation.
(50) Hafizovic Cavka, J.; Jakobsen, S.; Olsbye, U.; Guillou, N.; Lamberti, C.; Bordiga, S.; Lillerud, K. P. *J. Am. Chem. Soc.* **2008**, *130*, 13850–13851.
(51) Spoto, G.; Vitillo, J. G.; Cocina, D.; Damin, A.; Bonino, F.; Zecchina, A. *Phys. Chem. Chem. Phys.* **2007**, *9*, 4992–4999.

(52) Please note that the electrostatic potential of the [η^6-$C_6H_4(NH_2)_2$] molecule is not symmetric. In fact, the H pair of each $-NH_2$ group points out of the ring plane ($X_{barycenter\_of\_the\_H\_pair}-N-C = 134°$) in two opposite directions. The molecule has an inversion center in the "middle" of the benzene ring.

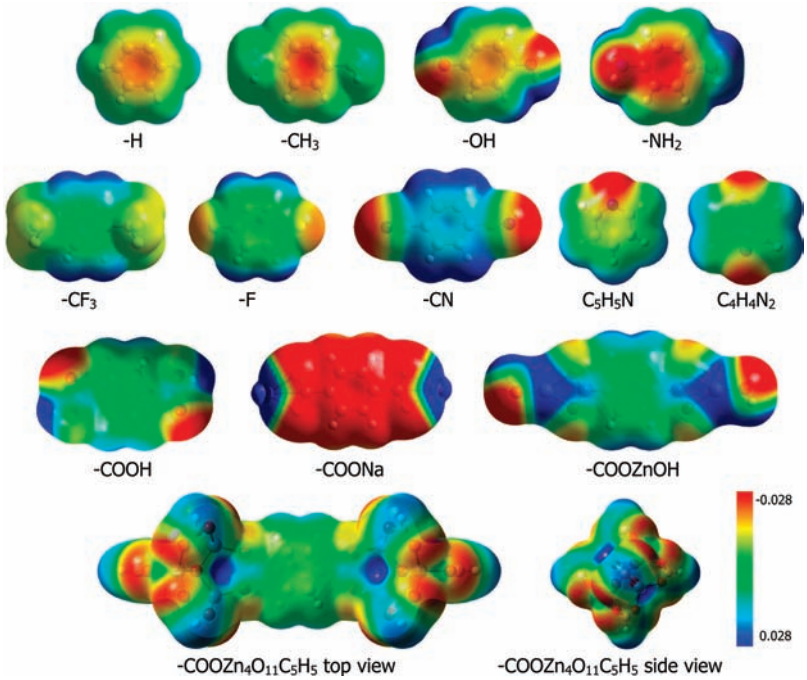

Figure 1. Electrostatic potential mapped on the 0.0004 isosurface of the total electron density as obtained at the B3LYP level for the arenes under study (reported in the same order as in Figure S1, Supporting Information). The electrostatic potential is represented with a color scale going from red (-2.8×10^{-2} au) to blue (2.8×10^{-2} au).

Table 1. Geometric (in Å), Energetic (in kJ mol^{-1}), and Vibrational (in cm^{-1}) Features of the (η^6-Arene)Cr(CO)$_3$ Complexes As Obtained at the B3LYP Level[a]

arene	Cr−C$_{CO}$[b]	Cr−arene[c]	Δ(C−O)[b,d]	D_e[d] (D_e)	D_0[d]	$\Delta H_{Cr(CO)_3}$[c,d]	$\Delta H_{Cr(CO)_6}$[c,d]	$\Delta\tilde{\nu}_{CO_{totsymm}}$	$\Delta\tilde{\nu}_{CO_{asymm}}$
C_6H_6	1.8624	1.7591	0.0254	201 (208)	193	−195	235	−156	−214/−214
$C_6H_4(CH_3)_2$	1.8585	1.7658	0.0268	210 (217)	200	−200	229	−166	−222/−227
$C_6H_4(OH)_2$	1.8586	1.7813	0.0265	192 (200)	185	−186	244	−162	−216/−228
$C_6H_4(NH_2)_2$	1.8535	1.7965	0.0286	206 (213)	198	−199	230	−173	−228/−246
$C_6H_4F_2$	1.8675	1.7593	0.0233	173 (180)	167	−167	262	−144	−198/−201
$C_6H_4(CN)_2$	1.8812	1.7378	0.0190	165 (171)	160	−160	270	−126	−167/−175
$C_6H_4(CF_3)_2$	1.8764	1.7387	0.0207	174 (181)	168	−168	261	−132	−178/−186
$C_6H_4(COOH)_2$	1.8746	1.7486	0.0213	184 (191)	178	−178	251	−138	−184/−191
$C_6H_4(COONa)_2$	1.8563	1.7746	0.0282	219 (227)	212	−213	217	−175	−233/−235
$C_6H_4(COOZnOH)_2$	1.8753	1.7469	0.0212	184 (192)	179	−179	251	−139	−184/−189
$C_6H_4(Zn_4O_{13}C_6H_5)_2$	1.8704	1.7534	0.0228	190 (198)	184	−184	245	−148	−197/−199
C_5H_5N	1.8682	1.7530	0.0231	177 (183)	170	−171	258	−142	−194/−204
$C_4H_4N_2$	1.8771	1.7369	0.0204	150 (156)	145	−146	284	−128	−175/−186

[a] The C_5H_5N complex is in the anti-eclipsed conformation. All of the other complexes are in the staggered conformation. [b] Average value. [c] Cr−arene: distance between Cr and the center of mass of the C (or N) atoms of the ring. [d] Δ(C−O): variation in the C−O bond length with respect to the free CO molecule. D_e: the dissociation energy from the potential energy minimum corresponding to eq 1. D_0: ZPE-corrected D_e. $\Delta H_{Cr(CO)_3}$: adduct formation enthalpy evaluated at 298.15 K and 1 atm (eq 1). $\Delta H_{Cr(CO)_6}$: standard enthalpy of the reaction reported in eq 2. $\Delta\tilde{\nu}_{CO_{totsymm}}$ and $\Delta\tilde{\nu}_{CO_{asymm}}$: shifts in the harmonic stretching frequency of the CO total-symmetric and asymmetric modes with respect to the free molecule. $q_{Cr(CO)_3}$: charge of the $CrCO_3$ unit in the complexes from Mulliken population analysis.

(or when just one heteratom is present), the latter can be either anti-eclipsed (c) or syn-eclipsed (d). The staggered conformation was confirmed to be the minimum conformation[20,33] for all of the complexes, except for those involving *p*-$C_6H_4(COONa)_2$ and C_5H_5N. Nevertheless, the $Cr(CO)_3$ unit is expected to be a free rotator at room temperature on the basis of the low barrier energies for the tripod rotation: 1.19 kJ mol^{-1} for C_6H_6, 1.49 kJ mol^{-1} for $C_6H_4(CN)_2$, 1.08 kJ mol^{-1} for $C_6H_4(OH)_2$, and 2.13 kJ mol^{-1} for $C_6H_4(CH_3)_2$ (B3LYP values).

In the case of *p*-$C_6H_4(COONa)_2$, the minimum conformation was the eclipsed one, even if the two conformers have a very similar energy (ΔE = 9.8 kJ mol^{-1}, B3LYP value, see Table S2). This different behavior is due to the mobility of the Na^+ cation that, after the $Cr(CO)_3$ complexation, moves from the original position in order to interact with the negatively charged O atoms of the $Cr(CO)_3$ unit. Because of this extra interaction energy, in this case, the eclipsed conformation corresponded to the global minimum. Because of the low difference in energy between the two conformations, the staggered results have been reported in the following for the sake of comparison with the other complexes. However, it is important to observe that the two [η^6-$C_6H_4(COONa)_2$]$Cr(CO)_3$ conformers were characterized by noticeably different IR spectra, because of the larger activation of the CO molecule in direct interaction with Na^+, which causes the appearance of a third largely red-shifted signal ($\Delta\tilde{\nu}_{CO}$ = −325 cm^{-1})

Table 2. Geometric (in Å), Energetic (in kJ mol^{-1}), and Vibrational (in cm^{-1}) Features of the (η^6-Arene)Cr(CO)$_3$ Complexes As Obtained at the BP86 Level[a]

arene	Cr−C$_{CO}$[b]	Cr-arene[b]	Δ(C−O)[b]	D_e[b](D_e)	D_0[b]	$\Delta H_{Cr(CO)_3}$[c, b]	$\Delta H_{Cr(CO)_6}$[c, b]	$\Delta\tilde{\nu}_{CO_{totsymm}}$	$\Delta\tilde{\nu}_{CO_{asymm}}$
C_6H_6	1.8480	1.7201	0.0283	244 (251)	237	−238	264	−140	−197/−197
$C_6H_4(CH_3)_2$	1.8450	1.7269	0.0297	252 (259)	244	−243	259	−149	−204/−208
$C_6H_4(OH)_2$	1.8445	1.7452	0.0296	235 (242)	228	−228	273	−146	−199/−211
$C_6H_4(NH_2)_2$	1.8403	1.7609	0.0320	249 (256)	242	−242	259	−159	−212/−228
$C_6H_4F_2$	1.8512	1.7247	0.0264	216 (223)	210	−210	291	−130	−184/−187
$C_6H_4(CN)_2$	1.8613	1.7088	0.0224	207 (214)	203	−203	299	−116	−160/−166
$C_6H_4(CF_3)_2$	1.8578	1.7084	0.0239	216 (224)	211	−211	290	−120	−169/−174
$C_6H_4(COOH)_2$	1.8567	1.7168	0.0246	226 (234)	222	−222	280	−126	−174/−179
$C_6H_4(COONa)_2$	1.8354	1.7361	0.0352	263 (271)	257	−257	245	−158	−216/−217
$C_6H_4(COOZnOH)_2$	1.8574	1.7155	0.0243	226 (234)	221	−221	281	−126	−173/−177
$C_6H_4(Zn_4O_{13}C_6H_5)_2$	1.8538	1.7206	0.0258	232 (241)	226	−226	275	−133	−183/−185
C_5H_5N	1.8522	1.7144	0.0260	220 (226)	214	−215	287	−127	−179/−188
$C_4H_4N_2$	1.8580	1.7044	0.0237	192 (198)	187	−188	314	−116	−166/−174

[a] The C_5H_5N complex is in the anti-eclipsed conformation. All of the other complexes are in the staggered conformation. [b] For the notation and units, see Table 1.

Scheme 2. Staggered (a), Eclipsed (b), Anti-Eclipsed (c), and Syn-Eclipsed (d) Conformers of the (η^6-Arene)Cr(CO)$_3$ Complexes[a]

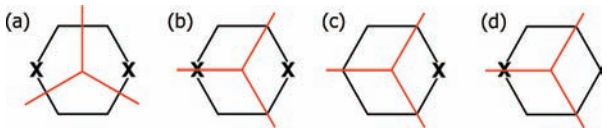

[a] The red lines represent the Cr(CO)$_3$ tripod. The X indicates the position of heteroatoms and/or of the C atoms of the ring bound to a substituent group.

not present in the staggered conformer spectrum (see section III.B.2 and Figure S3, Supporting Information).

For (η^6-C_5H_5N)Cr(CO)$_3$, the anti-eclipsed conformation was the energy minimum, as expected on the basis of the electron-withdrawing nature of the N heteroatom[53] and on previous X-ray diffraction data.[54] Since, in this case, it was not possible to optimize the complex in its staggered form, the reported results for (η^6-C_5H_5N)Cr(CO)$_3$ are for the anti-eclipsed conformation.

In conclusion, (i) all of the DFT-based functionals adopted in this work gave a qualitatively identical description of the (η^6-arene)Cr(CO)$_3$ complexes and the way their properties are influenced by changing the arene chemical nature (see Figures 3 and 4 and Figures S5 and S6, Supporting Information). (ii) The comparison with the experimental data, when available,[18,53,55−57] evidenced the ability of all of the methods to reproduce the geometrical features of the complexes within 0.04 Å. This was true in particular for the BP86 method, that showed the best agreement with the experimental structural values. The B3LYP method reproduced with larger accuracy the quadratic configuration interaction with single and double excitation Cr−ring distance for the C_6H_6 complex.[56] (iii) Most of the computed geometrical parameters were influenced by the HF proportion in the exchange functional. In particular, both the Cr−arene and the C−O distances decreased upon increasing X_{HF}, whereas the Cr−C_{CO} distance showed an opposite behavior. These trends on X_{HF} were also observed for the bare Cr(CO)$_3$ unit (see Table S1, Supporting Information). (iv) Finally, all of the methods indicated that the arene ring appears slightly distorted in the complex, especially at the site of the substituent, consistent with the observations of Hunter et al.[17,18] and the calculations of Lochan et al.[20] for the (η^6-arene)Cr(H_2)$_3$ complexes. In particular, the arenes assumed a "boat" or an "inverted boat" conformation for donor or acceptor substituents, respectively, in agreement with previous results.[17,18]

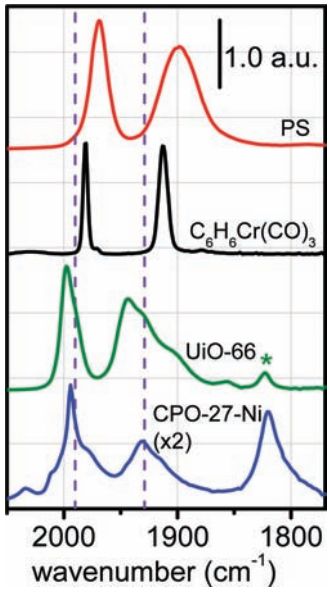

Figure 2. Comparison between FTIR spectra of the Cr(CO)$_3$ species grafted on different porous materials: a microporous poly(ethylstyrene-co-divinylbenzene) (red spectrum), UiO-66[50] (a MOF with no exposed metal sites, green spectrum), and CPO-27-Ni[59] (a MOF with exposed Ni^{2+} sites, blue spectrum). The two vertical lines referred to the maxima of the bands reported for the same species in MOF-5, as in ref 6. The spectrum of the (η^6-C_6H_6)Cr(CO)$_3$ compound in Nujol is also reported for comparison (black line). Note that the band at about 1820 cm^{-1} in the UiO-66 spectrum (labeled by an asterisk) is not related to the Cr(CO)$_3$ species, but it corresponds to a framework mode.[50]

III.B.2. Vibrational Properties. The ability of the methods to model the (η^6-arene)Cr(CO)$_3$ complexes has also

(53) Djukic, J. P.; Rose-Munch, F.; Rose, E.; Vaissermann, J. *Eur. J. Inorg. Chem.* **2000**, 1295–1306.
(54) Draper, S. M.; Byrne, J. J.; Breheny, C. J.; Long, C.; Low, J. N. *Acta Crystallogr., Sect. C* **1994**, *50*, 1669–1671.
(55) Jagirdar, B. R.; Klabunde, K. J.; Palmer, R.; Radonovich, L. J.; Williams, T. *Inorg. Chim. Acta* **1996**, *250*, 317–326.
(56) Low, A. A.; Hall, M. B. *Int. J. Quantum Chem.* **2000**, *77*, 152–160.
(57) Chiu, N.-S.; Schafer, L.; Seip, R. *J. Organomet. Chem.* **1975**, *10*, 331–346.

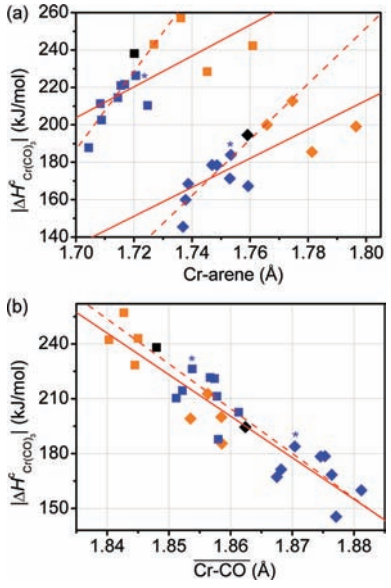

Figure 3. Dependence of $\Delta H_{Cr(CO)_3}{}^c$ on Cr−arene (a) and on the average Cr−CO distance (b) as obtained at the B3LYP (diamonds) and BP86 (squares) levels of calculations for the (η^6-arene)$Cr(CO)_3$ complexes. The blue symbols refer to the PA complexes (the asterisk indicates the $C_6H_4(Zn_4O_{13}C_6H_5)_2$ cluster), whereas the orange symbols refer to the NA ones. The black symbol refers to the benzene complex. The straight lines have been obtained (a) by separately fitting the BP86 and the B3LYP results and (b) by fitting them contemporaneously. The solid lines correspond to fits performed on all of the complexes, whereas the dashed lines refer to fits excluding the points related to $C_6H_4F_2$, $C_6H_4(OH)_2$, and $C_6H_4(NH_2)_2$ (see the text). For b, the solid line corresponds to $y = mx + q$, with $m = (-2273 \pm 200)$ kJ Å^{-1} mol^{-1}, $q = (4428 \pm 400)$ kJ mol^{-1}, and $r^2 = 0.8434$. The dashed line parameters are $m = (-2451 \pm 200)$ kJ Å^{-1} mol^{-1}, $q = (4765 \pm 400)$ kJ mol^{-1}, and $r^2 = 0.8900$. The parameters of the linear fits are reported in Tables S8 (solid lines) and S9 (dashed lines), see Supporting Information.

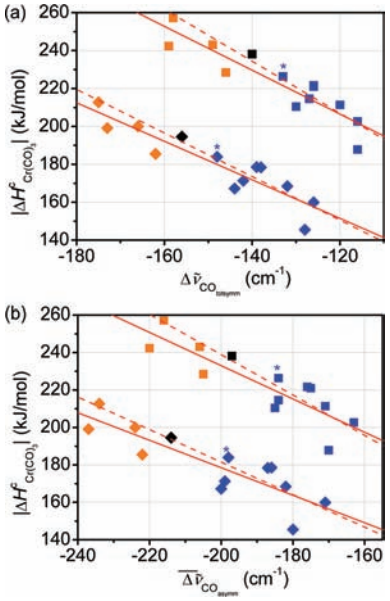

Figure 4. Dependence of $\Delta H_{Cr(CO)_3}{}^c$ on $\Delta\tilde{\nu}_{CO_{totsymm}}$ (a) and on the average $\Delta\tilde{\nu}_{CO_{asymm}}$ (b) as obtained at the B3LYP (diamonds) and BP86 (squares) levels of calculations for the (η^6-arene)$Cr(CO)_3$ complexes. Color code as in Figure 3. The straight lines have been obtained by separately fitting the BP86 and the B3LYP results. The parameters of the linear fits are reported in Tables S8 (solid lines) and S9 (dashed lines), see Supporting Information.

been checked by comparing the computed shift of the C−O vibrational frequency (with respect to the CO in the gas phase, $\Delta\tilde{\nu}_{CO}$) with the experimental values reported in the literature and obtained in our laboratories. A review of 22 $\Delta\tilde{\nu}_{CO}$ experimental values is presented in Table S3 of the Supporting Information. Generally speaking, the infrared spectra of the (η^6-arene)$Cr(CO)_3$ compounds (see Figure 2) are characterized in the 2100−1800 cm^{-1} region by one peak centered at about 2000 cm^{-1}, due to the total symmetric stretching of the three CO molecules ($\Delta\tilde{\nu}_{CO_{totsymm}}$) and a doublet (or a broad band) at about 1900 cm^{-1}, due to two asymmetric modes of the three CO's ($\Delta\tilde{\nu}_{CO_{asymm}}$). It is worth noticing that, with respect to the geometry, $\Delta\tilde{\nu}_{CO}$ is more sensitive to the balance between charge-transfer, exchange repulsion, and electrostatic interactions that are the three factors influencing the interaction between the arene and the $Cr(CO)_3$ moiety and between the Cr and the CO molecules. From the data reported in Table S3 (Supporting Information), it can be inferred that the CO frequencies of (η^6-arene)$Cr(CO)_3$ are significantly influenced not only by the nature of the arene but also by the chemical environment.[58] For example, the $\Delta\tilde{\nu}_{CO_{totsymm}}$ of (η^6-C_6H_6)$Cr(CO)_3$ changes from −144 cm^{-1} for the complex in the gas phase to −165 cm^{-1} in Nujol and −177 cm^{-1} in a KBr disk.[58]

(58) Wang, W.; Jin, P.; Liu, Y.; She, Y.; Fu, K. *J. Phys. Chem.* **1992**, *96*, 1278–1283.

The $|\Delta\tilde{\nu}_{CO}|$ value obtained by the different functionals was almost independent of the X_{HF} proportion, the BLYP, B3LYP, and BHandHLYP values differing in a range of 5 cm^{-1}. On the contrary, a significant difference was observed with the BP86 method, which in general underestimated $|\Delta\tilde{\nu}_{CO}|$ with respect to the LYP functionals (note that the same trend will be observed for the corresponding $|\Delta H_{Cr(CO)_3}|$, see below). All of the methods tend to underestimate the $\Delta\tilde{\nu}_{CO}$ shifts with respect to the experimental values, but they are all able to correctly reproduce the direction of the $\Delta\tilde{\nu}_{CO}$ change as a function of the ring substituent with respect to C_6H_6. In particular, the calculated $|\Delta\tilde{\nu}_{CO}|$ values are lower than those observed for the $C_6H_6Cr(CO)_3$ for arenes belonging to the PA set and greater for those of the NA complexes, in agreement with the trends of the C−O distance. The better agreement between theory and experiment was shown by the B3LYP functional, which was able to reproduce the $\Delta\tilde{\nu}_{CO_{totsymm}}$ with an accuracy of 10 cm^{-1} and the $\Delta\tilde{\nu}_{CO_{asymm}}$ within 20 cm^{-1}. The only exception was the $C_6H_4F_2$ complex, which showed very poor agreement at all levels of calculation: the methods were in fact able to correctly reproduce the red shift of CO bands with respect to $C_6H_6Cr(CO)_3$, but the difference between the calculated and the experimental values was very large (it amounts to 52 cm^{-1} for $\Delta\tilde{\nu}_{CO_{asymm}}$ and to 27 cm^{-1} for $\Delta\tilde{\nu}_{CO_{totsymm}}$ at the B3LYP level). Nevertheless, this difference could be more likely due to the difference between the chemical environments in the calculation (gas phase) and in the experiment (CH_2Cl_2 solution)[55] than to a lack of the computational methods.

The dependence of $\Delta\tilde{\nu}_{CO}$ on the nature of the substituent ligand suggested by theoretical calculations has been further demonstrated by experimental results. In fact, expanding the idea of Kaye and Long for

MOF-5,[6] in our laboratories, some of us have succeeded in grafting a $Cr(CO)_3$ tripod on a microporous poly(ethylstyrene-*co*-divinylbenzene)[49] and on two MOF materials: UiO-66,[49,50] a MOF with no exposed metal sites, and CPO-27-Ni,[49] a MOF material with exposed Ni^{2+} sites. The infrared spectra of the $Cr(CO)_3$-grafted materials are reported in Figure 2. For comparison, the spectrum of the pure $(\eta^6\text{-}C_6H_6)Cr(CO)_3$ compound is also reported (black curve). It is evident that the CO bands are very sensitive to the nature of the supporting material: in particular, a blue shift with respect to the pure $(\eta^6\text{-}C_6H_6)Cr(CO)_3$ was observed for MOF-5[6] and UiO-66, whereas a red shift of the bands was obtained for the $Cr(CO)_3$ grafted in PS. The computational data discussed above can help in explaining the experimental red or blue shift of the $\Delta\tilde{\nu}_{CO}$ bands, in terms of the electron-donor or electron-acceptor nature of the ring substituents. In particular, the red shift of the $\Delta\tilde{\nu}_{CO}$ bands (-13 and $-14\ cm^{-1}$ for $\Delta\tilde{\nu}_{CO_{totsymm}}$ and $\Delta\tilde{\nu}_{CO_{asymm}}$, respectively) observed in PS with respect to the pure $(\eta^6\text{-}C_6H_6)Cr(CO)_3$ (see Figure 2) can be explained in terms of the electron-donor nature of the ring substituents. In a first approximation, in fact, the ethylbenzene unit contained in this polymer can be modeled by the $C_6H_4(CH_3)_2$ cluster (NA set), for which a shift of -10 and $-13\ cm^{-1}$ was obtained (B3LYP results) with respect to the $(\eta^6\text{-}C_6H_6)Cr(CO)_3$ complex. Modeling the UiO-66 material with the $C_6H_4(COOH)_2$ cluster allowed for a nice explanation of the blue shift of the CO bands in the corresponding experimental spectrum (green curve). Finally, the experimental $\Delta\tilde{\nu}_{CO}$ bands reported for MOF-5 material[6] (dashed lines) were blue-shifted with respect to $(\eta^6\text{-}C_6H_6)Cr(CO)_3$ by $+9$ and $+16\ cm^{-1}$, respectively; these shifts well agree with the $+8$ and $+16\ cm^{-1}$ values calculated by B3LYP for $C_6H_4(Zn_4O_{13}C_6H_5)_2Cr(CO)_3$ (PA set). The difference between the computed CO shifts obtained for $C_6H_4(Zn_4O_{13}C_6H_5)_2Cr(CO)_3$ and $C_6H_4(COOH)_2Cr(CO)_3$ was unexpected on the basis of the coincidence of the experimental values for $[MOF\text{-}5]Cr(CO)_3$ and $C_6H_4(COOH)_2Cr(CO)_3$ reported in ref 6. However, this difference can be related once more to the difference in the $C_6H_4(COOH)_2Cr(CO)_3$ chemical environment in the experiment (bulk phase) and in the calculations (gas phase).

Note that the $\Delta\tilde{\nu}_{CO_{totsymm}}$ and the $\Delta\tilde{\nu}_{CO_{asymm}}$ bands of the $Cr(CO)_3$ species in both PS and UiO-66 samples are characterized by a larger full-width at half-maximum (fwhm) with respect to the pure $(\eta^6\text{-}C_6H_6)Cr(CO)_3$, even if the relative ratio of the fwhm's of the two bands is basically the same. This evidence suggests a higher heterogeneity of species in the two investigated supports.

A more complex situation occurs in the case of $[CPO\text{-}27\text{-}Ni]Cr(CO)_3$ where, together with the two components in the $2100-1900\ cm^{-1}$ range, a new band appeared at a lower frequency ($1820\ cm^{-1}$). The presence of this component suggests the rupture of the quasi-degeneracy of the asymmetric stretching modes due to the interaction of the CO molecules with the exposed Ni^{2+} ions. It has been experimentally demonstrated that metal−carbonyls, where the O atom of the CO interacts directly with the positive center, experience larger $|\Delta\tilde{\nu}_{CO}|$ values.[60] The computed spectra of the $[\eta^6\text{-}C_6H_4(COONa)_2]Cr(CO)_3$ model in the staggered and eclipsed conformations are compared in Figure S3 (parts a and b, respectively; see also Table S2, Supporting Information). It is evident that the spectrum of the eclipsed conformer shows a decidedly red-shifted band ($\Delta\tilde{\nu}_{CO} = -325\ cm^{-1}$) that is absent in the spectrum of the staggered conformer; this band is due to the simultaneous interaction of one CO molecule with the Cr center (through the C atom) and the Na^+ center (through the O atom). The corresponding $\Delta\tilde{\nu}_{CO}$ is in fair agreement with that of the most red-shifted band in $[CPO\text{-}27\text{-}Ni]Cr(CO)_3$ ($\Delta\tilde{\nu}_{CO} = -323\ cm^{-1}$), supporting the hypothesis that this band is originated by the direct interaction of one CO of the tripod with the exposed Ni^{2+} ion through the O atom.

III.B.3. Stability. Thermodynamic aspects of the stability of these complexes were the subject of the refs 61−67. The computed $\Delta H_{Cr(CO)_6}^{c}$ values always exceed 200 kJ/mol (see Tables 1 and 2), indicating that the formation of the $(\eta^6\text{-arene})Cr(CO)_3$ complexes following eq 2 is unfavored under standard conditions. This agrees with the long reaction time and the high temperature needed to graft $Cr(CO)_3$ on MOFs and polymers from $Cr(CO)_6$ (see ref 6 and section II.B). A great stability of the $(\eta^6\text{-arene})Cr(CO)_3$ complexes once formed can be, on the contrary, expected on the basis of the high values obtained for $|\Delta H_{Cr(CO)_3}^{c}|$ (eq 1), indicating a strong interaction between the $Cr(CO)_3$ moiety and the ring. For the benzene complex, it was possible to compare the computed $|\Delta H_{Cr(CO)_3}^{c}|$ (184 for BLYP, 194 for B3LYP, 187 for BHandHLYP, and 238 kJ/mol for BP86) with the corresponding experimental value (222 kJ/mol),[68] confirming the ability of the DFT methods to reproduce the features of the complexes under investigation. In particular, the LYP methods underestimate the experimental value, while BP86 overestimates it. In all cases under investigation, the $|\Delta H_{Cr(CO)_3}^{c}|$ values obtained by the LYP family of methods were always lower than the corresponding BP86 values, but by an almost constant value (49−55 for BLYP, 42−44 for B3LYP, and 46−53 kJ/mol for BHandHLYP). This allows for confidence in the computed results and in particular in the qualitative indications that can be deduced from them.

III.C. Comprehensive Analysis of Energetic, Geometric, and Vibrational Data. Once the reliability of DFT calculations was demonstrated, the possibility to obtain indications

(59) Bonino, F.; Chavan, S.; Vitillo, J. G.; Groppo, E.; Agostini, G.; Lamberti, C.; Dietzel, P. D. C.; Prestipino, C.; Bordiga, S. *Chem. Mater.* **2008**, *20*, 4957–4968.
(60) Otero Areán, C.; Tsyganenko, A. A.; Escalona Platero, E.; Garrone, E.; Zecchina, A. *Angew. Chem., Int. Ed.* **1998**, *37*, 3161–3163.
(61) Adedeji, F. A.; Lalage, D.; Brown, S.; Connor, J. A.; Leung, M. L.; Paz-Andrade, I. M.; Skinner, H. A. *J. Organomet. Chem.* **1975**, *97*, 221–228.
(62) Traylor, T. G.; Stewart, K.; Goldberg, M. *J. Am. Chem. Soc.* **1984**, *106*, 4445–4454.
(63) Muetterties, E. L.; Bleeke, J. R.; Sievert, A. C. *J. Organomet. Chem.* **1979**, *178*, 197–216.
(64) Solladié-Cavallo, A. *Polyhedron* **1985**, *4*, 901–927.
(65) Strohmeier, W.; Mittnacht, H. *Z. Phys. Chem. (Wiesbaden)* **1961**, *29*, 339–346.
(66) Strohmeier, W.; Muller, R. *Z. Phys. Chem. (Wiesbaden)* **1964**, *40*, 85–95.
(67) Mahaffy, C. A. L.; Pauson, P. L. *J. Chem. Res. Synop.* **1979**, *126 (M)*, 1752–1775.
(68) Mukerjee, S. L.; Lang, R. F.; Ju, T.; Kiss, G.; Hoff, C. D. *Inorg. Chem.* **1992**, *31*, 4885–4889.

of the relative stability of the grafted $Cr(CO)_3$ species from spectroscopic or structural data was investigated. Indeed, the experimental determination of $\Delta\tilde{\nu}_{CO}$ or of Cr−CO and Cr−arene distances is more immediate than the calorimetric measurement of $\Delta H_{Cr(CO)_3}{}^{c}$ that constitutes a more complicated task.[68] Figures 3 and 4 report the dependence of the calculated $\Delta H_{Cr(CO)_3}{}^{c}$ on Cr−arene and $Cr-C_{CO}$ distances and on $\Delta\tilde{\nu}_{CO}$, respectively (in the B3LYP and BP86 cases). It is evident that, with the exception of the $\Delta H_{Cr(CO)_3}{}^{c}$ versus Cr−arene plot, a good linear correlation exists between $\Delta H_{Cr(CO)_3}{}^{c}$ and the structural and vibrational features. The plots also visualize the great similarity of the relative complexes' descriptions given by the different DFT functionals.

All of the complexes belonging to the PA (blue symbols) or the NA (orange symbols) sets show a common behavior with respect to what is observed for (η^6-C_6H_6)-$Cr(CO)_3$ (black symbol). For the case of $|\Delta H_{Cr(CO)_3}{}^{c}|$, it is evident that, when the ring is less electron-rich than C_6H_6 (because of the presence of an electron acceptor or electronegative heteroatoms, PA complexes), the $|\Delta H_{Cr(CO)_3}{}^{c}|$ value is lower than that for C_6H_6 (that is, the complex is less stable); correspondently, the $\Delta H_{Cr(CO)6}$ is higher (that is, it is more difficult to graft $Cr(CO)_3$ on the ring from the point of view of the overall change in enthalpy, see Tables S4−S7, Supporting Information). It is worth notice that the model clusters of MOF-5 belong to this set. For the rings substituted with electron-donor groups, the opposite behavior is observed as expected, except for the 1,4-dihydroxybenzene. This deviation agrees with what was evidenced by the electrostatic maps; in fact, although characterized by negative values of the ESP on the ring, this arene is characterized by ESP values more positive than those obtained for C_6H_6 (see previous section, Figure 1).

The π-donor or π-acceptor nature of the arene's substituents in (η^6-arene)$Cr(CO)_3$ complexes influenced their structural properties, as demonstrated by a systematic X-ray crystallographic study conducted by Hunter et al.[17,18] This was confirmed by the calculations performed in the present study; in particular, the Cr−arene distances were in general larger than in the benzene complex for the NA set and shorter for complexes belonging to the PA set (with the exception of $C_6H_4F_2$, see below). This was unexpected on the basis of the $\Delta H_{Cr(CO)_3}{}^{c}$ values, which indicated a larger stability of the NA complexes with respect to (η^6-C_6H_6)$Cr(CO)_3$. However, this observation is in agreement with computational results obtained by Lochan et al.[20] for the (η^6-arene)$Cr(H_2)_3$ complexes. Moreover, the larger Cr−arene distance of the NA complexes could be easily explained if the different electron density on the rings is taken into account; in fact, a larger electron density of the NA rings with respect to C_6H_6 implies a large Cr−arene distance due to a greater electronic repulsion. The Cr−CO distance follows the opposite trend of Cr−arene; it is larger than in the benzene complex for the PA and shorter for the NA complexes. This agrees with what is expected on the basis of the ESP maps and the $\Delta H_{Cr(CO)_3}{}^{c}$ values, which indicates a larger back-donation to the CO (and then a stronger Cr−CO bond) for the NA complexes. Accordingly, the elongation of the C−O distance was found to be larger for NA complexes than in (η^6-C_6H_6)$Cr(CO)_3$, whereas in PA a smaller elongation was observed. This is in agreement with the experimental observation.[17,18] On this basis, it is expected that CO substitution by more weakly interacting molecules would be easier on a thermodynamic basis for MOFs having linkers belonging to the PA set. This agrees with the findings reported in the recent study of Lochan et al.[20]

As far as the $\Delta H_{Cr(CO)_3}{}^{c}$ dependence on the structural features is concerned, a linear correlation between $\Delta H_{Cr(CO)_3}{}^{c}$ and Cr−arene or Cr−CO distances was evidenced for all of the methods (see, for example, Figure 3). The linear regression results are almost coincident in the error (see Tables S8−S11, Supporting Information). This suggests that an indication of the relative stability of (η^6-arene)$Cr(CO)_3$ complexes could be effectively obtained from structural data (e.g., from XRD or extended X-ray absorption fine structure (EXAFS) analysis).

A good linear dependence was found also between $\Delta H_{Cr(CO)_3}{}^{c}$ and $\Delta\tilde{\nu}_{CO_{totsymm}}$ and between $\Delta H_{Cr(CO)_3}{}^{c}$ and $\Delta\tilde{\nu}_{CO_{asymm}}$, even better than that obtained for the structural parameters, as shown in Figure 4 and Tables S8 and S9 (Supporting Information). As already evidenced for the structural parameters, the interpolation of the data obtained by different methods results in similar slopes, allowing good confidence in the obtained results. Because of that and for the goodness of the linear fit ($0.7 < r^2 < 0.86$), it can be affirmed that an indication of the complex stability could be also obtained from a comparison of the $|\Delta\tilde{\nu}_{CO}|$ values (that is, from IR spectroscopy). Because a linear dependence exists also between $\Delta H_{Cr(CO)_3}{}^{c}$ and the Cr−CO distance, indications on the relative Cr−CO bond strength can be deduced from the IR spectrum of these compounds (the larger the $|\Delta\tilde{\nu}_{CO}|$, the smaller the Cr−CO distance).

For all of the graphs reported in Figures 3–4, the goodness of the linear fits increases significantly if the points related to the $C_6H_4F_2$, $C_6H_4(OH)_2$, and $C_6H_4(NH_2)_2$ clusters are omitted (this can emerge from the comparison of the r^2 values in Tables S8 and S9, Supporting Information). The new linear regression results are reported as dashed lines in the plots. The increase in the fit quality is particularly evident for the $|\Delta H_{Cr(CO)_3}{}^{c}|$ versus Cr−arene plot (see Figure 3a); in this case, the effects are drastic not only on the correlation coefficient values (that increased from 0.5 to 0.9) but also on both the slope and the intercept of the straight lines. The deviations of $C_6H_4(OH)_2$ and $C_6H_4(NH_2)_2$ from the common behavior can be ascribed to the interaction of the substituents with the tripod in such complexes. In particular, for both $C_6H_4(OH)_2$ and $C_6H_4(NH_2)_2$, the position of the H atoms of the −OH and $-NH_2$ groups changes significantly in the $Cr(CO)_3$ complexes from that in the bare arenes. These H atoms (positively charged, Figure 1) tilt in order to minimize the distance from the O atoms of the tripod (negatively charged, Figure S2, Supporting Information). This effect is not present in other complexes, for example, in that of $C_6H_4(COOH)_2$, because of the larger distance between the positively charged atoms of the substituents and the tripod or because of their lower mobility. This has a direct influence on the Cr−arene properties because, for steric effects, the $Cr(CO)_3$ distance has to be larger than that expected on the basis of

the $\Delta H_{Cr(CO)_3}{}^{c}$. Moreover, if on one hand the presence of such interaction is expected not to have an important influence on $\Delta H_{Cr(CO)_3}{}^{c}$, on the other it is expected to have a more drastic effect on $|\Delta\tilde{\nu}_{CO}|$, because of the interaction through the O atoms (see Figure S3, Supporting Information). In fact, a quick look at Figure 4 reveals that the $|\Delta\tilde{\nu}_{CO}|$ values are larger than those expected on the basis of the $\Delta H_{Cr(CO)_3}{}^{c}$ values.

Finally, for the case of the $C_6H_4F_2$ complex, the C−F carbons are, on the contrary, moved further away from the Cr center, according to the acceptor nature of the −F substituents. This agrees with what was reported by Jagirdar et al.,[55] who observed this slight folding also in *p*-$(C_6H_4F_2)Cr(CO)_2(SiCl_3)_2$ and attributed it to the significant negative charge present on the F atoms (−0.305851*e* Mulliken charge according to B3LYP for the bare arene) and to the corresponding electron repulsion with the O atoms of the $Cr(CO)_3$ unit, also due to the large anionic radius of the F center. This would result in a Cr−arene distance larger than that obtained for benzene. However, the C atoms in the ortho position are more negative than the C atoms in benzene, so that they are attracted by the positive Cr center (as expected for an acceptor-substituted benzene for which a Cr−arene distance shorter than the benzene one is predicted). The two effects are compensating for each other, and the resulting Cr−arene distance is only slightly larger than that for benzene (of 0.0046 and 0.0003 Å at the BP86 and B3LYP levels, respectively), different from what occurs for the other PA complexes.

IV. Conclusions

The possibility to modulate the properties of $Cr(CO)_3$ by grafting it onto MOF linkers of different natures has been investigated by different density functional methods. In particular, the effect of the electron-donor or electron-acceptor nature of benzene substituents and of heteroatoms in the ring on the stability of the (η^6-arene)$Cr(CO)_3$ adducts and on their structural and vibrational properties has been considered. All of the functionals adopted were able to correctly predict the structures of such complexes; in particular, BP86 gave the structural and energetic description of the complexes nearest to the experimental one, whereas the B3LYP functional was the method able to give the most precise description of the CO vibrational shifts.

The modulation of the stability and the reactivity of grafted $Cr(CO)_3$ species by properly choosing the MOF on the basis of its organic linker was so verified. In particular, this study indicated that arenes with positive values of the electrostatic potential on the ring (C_5H_5N and $C_4H_4N_2$ and electron-acceptor substituted rings as the common MOFs linker, $C_6H_4(COOH)_2$) have to be chosen in order to facilitate the substitution of CO by more weakly interacting molecules (one of the possible methods of the hydrogen storage). On the contrary, arenes with negative ESP values on the rings (as electron-donor substitutes benzene, e.g., $C_6H_4(CH_3)_2$ or $C_6H_4(OH)_2$) would improve the stability of the $Cr(CO)_3$ adduct and the ring acidity.

Furthermore, an almost linear dependence of the $Cr(CO)_3$ binding energies on the calculated structural and vibrational features of the tripod was found, suggesting that indications about the stability of the $Cr(CO)_3$ adduct can be derived from FTIR spectroscopy and diffraction or EXAFS data. Therefore, the coupling of theoretical calculations and experimental measurements allows for the prediction and checking of some key parameters in the design of gas storage materials and catalysts. Finally, on the basis of the results obtained, it was possible to explain the reasons for the experimental blue/red shift of the CO IR stretching features with respect to the bare (η^6-C_6H_6)$Cr(CO)_3$ for $Cr(CO)_3$ grafted on the UiO-66, CPO-27-Ni, and MOF-5 aromatic linkers and on the benzene rings of poly(ethylstyrene-*co*-divinylbenzene). The sign of the $\Delta\tilde{\nu}_{CO}$ shift has been found to be strongly dependent on higher and lower electron densities of the ring with respect to the C_6H_6 complex.

Acknowledgment. Financial support by Regione Piemonte in the frame of the research project "Innovative materials for hydrogen storage" and by European VI framework through STREP project MOFCAT, contract number NMP4-CT-2006-033335 is gratefully acknowledged. Dr. Alessandro Damin is kindly acknowledged for fruitful discussions. Dr. M. J. Uddin is acknowledged for providing the (η^6-C_6H_6)$Cr(CO)_3$ spectrum in Nujol. Prof. K. P. Lillerud is acknowledged for kindly providing the UiO-66 material. Dr. P. D. C. Pascal is acknowledged for kindly providing the CPO-27-Ni material.

Supporting Information Available: Figure of the arene models as optimized at the B3LYP level, geometrical and vibrational and electrostatic properties of the $Cr(CO)_3$ and $Cr(CO)_6$ molecules as obtained at all the levels of calculation, details of the eclipsed $[C_6H_4(COONa)_2]Cr(CO)_3$ structure as calculated at the B3LYP and BP86 levels, review of experimental $\Delta\tilde{\nu}_{CO}$ for (η^6-arene)$Cr(CO)_3$ complexes, full comprehensive tables for all of the methods, linear regression results for the BLYP and BHandHLYP methods, and atomic coordinates of all of the clusters as obtained at the B3LYP level. This material is available free of charge via the Internet at http://pubs.acs.org.